Spin Polarized Tunneling at Finite Bias

S. O. Valenzuela, D. J. Monsma, C. M. Marcus, V. Narayanamurti, and M. Tinkham
Gordon McKay Laboratory, Harvard University, Cambridge, Massachusetts 02138, USA
(Received 13 May 2004; published 16 May 2005)

A mesoscopic spin valve is used to determine the dynamic spin polarization of electrons tunneling out of and into ferromagnetic (FM) transition metals at finite voltages. The dynamic polarization of electrons tunneling *out of* the FM slowly decreases with increasing bias but drops faster and even inverts with voltage when electrons tunnel *into* it. A free-electron model shows that in the former case electrons originate near the Fermi level of the FM with large polarization whereas in the latter, electrons tunnel into hot electron states for which the polarization is significantly reduced. The change in sign is ascribed to the matching of the electron wave function inside and outside the tunnel barrier.

DOI: 10.1103/PhysRevLett.94.196601 PACS numbers: 72.25.Ba, 72.25.Hg, 75.70.-i, 85.30.Mn

Pioneering experiments by Meservey and Tedrow [1] richly contributed to the understanding of spin polarized tunneling from ferromagnetic (FM) materials. These experiments were performed using a superconducting counterelectrode [1] as a spin detector and, for this reason, were constrained to cryogenic temperatures (< 1 K) and ''zero''-bias measurements (< 1 mV). The subsequent development of magnetic tunnel junctions (MTJs) consisting of FM-I-FM structures [2] (I is an insulator) and the observation of the tunneling magnetoresistance (TMR) attracted much interest due to possible applications in the magnetic sensor and memory industry. From a fundamental point of view, MTJs offered the possibility of studying spin polarized tunneling without the constraints of low temperatures and low bias [2–7]. The analysis of the TMR is, however, complicated because it involves electrons tunneling *out of* one ferromagnetic electrode (cathode) *into* another (anode) and the spin polarizations of both electrodes participate. Experimental results [2–5], which consistently show a decrease in the TMR as a function of bias, are controversial and no consensus has been reached on the physics behind them. A measurement which discriminates the influence of each electrode is essential to gain further insight into their role in the TMR and into spin polarized tunneling in general. Such a technique would offer information on the nature of the tunneling electrons *out of* and *into* a FM and would be important for both scientific and technological reasons.

In this Letter, we determine the voltage dependence of the tunneling spin polarization up to voltages near the breakdown of the tunnel junctions using mesoscopic spin valves with the Johnson and Silsbee geometry [8–10]. This is done at both 4 and 295 K. We find that the dynamic spin polarization of the electrons tunneling *out of* the ferromagnet (FM acting as a cathode) is weakly voltage dependent but drops strongly and even inverts when tunneling *into* it (FM acting as an anode). By means of a free-electron model, we show that electrons tunneling out of the FM originate below the Fermi level with relatively large polarization, whereas electrons tunneling into the FM face hot electron states with decreasing polarization. Our calculations demonstrate that, in the latter case at high bias, spin polarization can change sign due to wave-vector matching effects in the transmission probability. These experimental and theoretical findings are important to qualitatively understand the bias dependence of the tunneling magnetoresistance in magnetic tunnel junctions.

We prepare our devices [Fig. 1(a)] with electron beam lithography and a three-angle shadow evaporation technique to produce tunnel barriers *in situ* [11]. An aluminum (Al) strip (100–150 nm wide and 6 nm thick) is first deposited through a suspended mask onto a Si/SiO_2 substrate using *e*-beam evaporation. Next, the aluminum is oxidized in pure oxygen (150 mTorr for 20 min) to generate insulating Al_2O_3 barriers. After pumping again, two 60–80 nm wide FM electrodes with different coercive fields are deposited sequentially from two different angles (CoFe and NiFe, 20 and 35 nm thick, respectively). They form tunnel junctions where they overlap with the Al strip

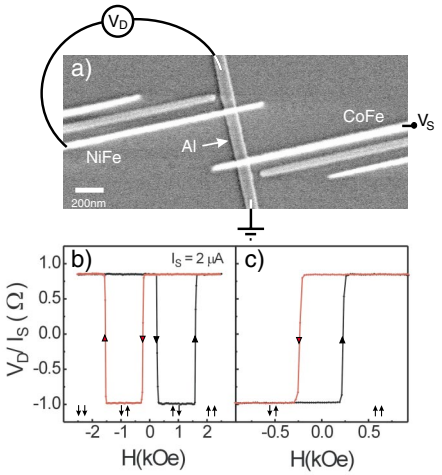

FIG. 1 (color online). (a) Scanning electron microscope image of a device and measuring scheme. (b),(c) Spin-valve effect. V_D/I_S for $V_{dc} = 0$ and $I_S = 2$ μA as a function of H at 4.2 K. The arrows on the curves indicate the field sweep direction. The arrows at the bottom of the figure represent the magnetic configuration of the leads.

with a typical tunnel resistance of about 50 kΩ. The distance d between the FM electrodes was varied from 150 to 1000 nm. We show data for $d = 220$ nm.

One of the FM electrodes sources spin polarized carriers to the Al strip through the Al_2O_3 tunnel barrier. A voltage V_S on the ''source'' [CoFe in Fig. 1(a)] generates a current I_S. For $V_S < 0$, electrons tunnel out of the FM, whereas for $V_S > 0$ the electrons tunnel into it. The effective polarization of the source is, by definition, the polarization of the tunneling electrons which is equal to $P_S = \frac{I_{\mathrm{maj}} - I_{\mathrm{min}}}{I_S}$, where $I_{\mathrm{maj,min}}$ are the tunneling currents for the majority- and minority-spin electrons and $I_S = I_{\mathrm{maj}} + I_{\mathrm{min}}$ is the total current (assuming independent spin channels). The polarized current results in a nonequilibrium spin accumulation in the Al strip which is determined by means of a second FM electrode [NiFe in Fig. 1(a)] with effective polarization P_D. The output voltage V_D between this ''detector'' and the Al strip is related to the spin degree of freedom, and it has been shown to be proportional to I_S and the polarizations of the electrodes; i.e., $V_D \propto P_D P_S I_S$ [9,10]. The sign of V_D depends on the relative configuration of the FM magnetizations.

Since the detector is not biased in our experiments, P_D stays constant. Thus, when $I_S(V_S)$ is modified, V_D follows the resulting change in the populations of the majority and minority electrons tunneling out of/into the source ($V_D \propto P_S I_S = I_{\mathrm{maj}} - I_{\mathrm{min}}$), which is the property we want to study. Note that the roles of the FM electrodes are interchangeable and that the bias characteristics of the polarized tunneling of both CoFe and NiFe can be analyzed.

The measurements were performed using lock-in techniques by applying a bias voltage $V_S = V_{\mathrm{dc}} + V_{\mathrm{ac}}$ to the source junction and measuring the output ac voltage at the remote detector. Figure 1(b) shows a typical spin-valve signal V_D/I_S at 4.2 K and $V_{\mathrm{dc}} = 0$ as a function of an applied in-plane magnetic field H along the axis of the FMs (CoFe was used as the source). At large enough negative H the magnetizations of the FMs point to the same direction (parallel configuration). As H is swept from negative to positive, a change in the sign of the detector signal is observed at 0.25 kOe when the magnetization of the electrode with the lower coercive field (NiFe) reverses and the device switches to an antiparallel configuration. As H is further increased, the CoFe electrode flips (at 1.5 kOe) and a parallel configuration is recovered. Figure 1(b) also shows V_D/I_S while sweeping down H. In this case, the antiparallel configuration is found between -0.25 and -1.5 kOe. At $H = 0$, the configuration of the electrodes is always parallel in these measurements. However, Fig. 1(c) shows that both configurations are possible at $H = 0$ and that they can be prepared in a controlled way. The antiparallel configuration is achieved by reversing the sweep direction of H when only the NiFe has switched.

From the output voltage difference between the two configurations as a function of d, we estimated the (low bias) polarization of the electrodes to be of the order of 25% at 4.2 K [11]. The larger polarization and the reduction of sample dimensions by an order of magnitude, in particular, the distance between the FMs and the Al thickness, help increase the detected signal by a factor of 200 as compared to Ref. [10]. This allows us to perform sensitive dc-voltage-dependent measurements. In this case, the source junction is excited with both dc and ac voltages. The small ac voltage (30 mV) is used to sense the variation of the polarization as a function of V_{dc}.

In order to follow changes in the transmission of majority- and minority-spin electrons as a function of bias, we measure the *dynamic* polarization defined as $p = (G_{\mathrm{maj}} - G_{\mathrm{min}})/(G_{\mathrm{maj}} + G_{\mathrm{min}})$ [12], where $G_{\mathrm{maj,min}}$ (which are V_{dc} dependent) are the *dynamic* conductances of the majority and minority electrons and $G_{\mathrm{maj}} + G_{\mathrm{min}}$ is the total dynamic conductance of the source junction. The difference in the output ac voltage between the two configurations of the FMs is proportional to the derivative of the output signal V_D introduced above with respect to V_{dc}; i.e., it is proportional to $\frac{d(P_S I_S)}{dV_{\mathrm{dc}}} = \frac{d(I_{\mathrm{maj}} - I_{\mathrm{min}})}{dV_{\mathrm{dc}}} = G_{\mathrm{maj}} - G_{\mathrm{min}}$. This implies that we can experimentally obtain p by simply dividing this difference in the output voltage by the dynamic conductance of the source junction [shown in Fig. 2(c) for CoFe]. Measurements were performed by preparing the sample in each of the two states of Fig. 1(c) at $H = 0$ and then sweeping V_{dc}.

The main experimental results are shown in Fig. 2. Figure 2(a) shows p (normalized at $V_{\mathrm{dc}} = 0$) as a function of V_{dc} ($T = 4.2$ K). The black symbols are for CoFe as the source, whereas the gray symbols are for NiFe. The inset shows the results for a second sample at 295 K. The same bias dependence of p is observed for these two samples and for four other samples not presented here with variable distances between source and detector.

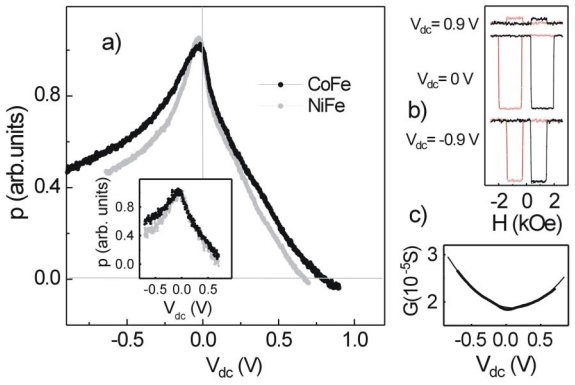

FIG. 2 (color online). (a) Normalized dynamic polarization p for a sample at 4.2 K (main panel) and a sample at 295 K (inset). Electrons are injected out of the FM for $V_{\mathrm{dc}} < 0$ and into it for $V_{\mathrm{dc}} > 0$. (b) Spin-valve effect showing a sign change in the voltage switching at large positive bias (CoFe as the source). (c) Dynamic conductance of the CoFe junction at 4.2 K.

The results are qualitatively the same for CoFe and NiFe. For negative dc biases, electrons are injected out of the source electrode into the Al strip. The resulting signal, shown in Fig. 2(a), reaches a maximum around -50 mV and then drops, but even for the largest negative applied voltages, it is still of comparable magnitude to the one at zero bias. On the other hand, for positive bias, when electrons are injected out of the Al into the FM, the dynamic polarization drops faster. At $V_{dc} = +0.5$ V, the detector signal has decreased significantly; it reaches zero at approximately $+0.8$ V($+0.67$ V) for CoFe (NiFe), and it is clearly negative for larger biases. Figure 2(b) shows the output voltage as H is swept for different fixed values of V_{dc} (CoFe as source). At $V_{dc} = +0.9$ V, the sign change in the voltage switching is clearly seen [13]. From the definition of p, this implies that, around this bias, the dynamic conductance for minority electrons dominates.

Using a free-electron model, we calculate the spin currents in a FM-Al_2O_3-Al (source) junction versus bias and discuss how these results are related to the experiments above and to the magnetoresistance in MTJs. In our model we extend Gundlach's approach [14] to include two independent spin currents. The current through the barrier at finite bias $I(V_{dc})$ is obtained from the bias-dependent transmission probability, $D(eV_{dc}, E)$, for tunneling electrons with energy E. D is found by exactly solving the Schrödinger equation for parabolic free-electron energy bands and a trapezoidal shape tunnel barrier [Fig. 3(a)] using the Airy wave function solutions within the tunnel barrier. $I(V_{dc})$ is found integrating D over E as discussed in Ref. [14], for each spin band. The FM is characterized by an exchange-split parabolic energy band, which results in majority and minority bands with distinct energies E_{maj} and E_{min} for the bottom of the bands below the Fermi energy. It is likely that the tunneling electron will have significant s-p character and thus a free-electron-like dispersion relation ($E \propto k^2$) is justified [6,15].

Since spin-flip scattering is neglected, the total current is comprised of two independent electron-tunneling currents associated with the two spin populations. For the negatively biased FM-Al_2O_3-Al junction, the current is $I = I_{maj\to unp} + I_{min\to unp}$, where $I_{maj(min)\to unp}$ is the current from the majority (minority) band to the unpolarized band in the normal metal (Al in our experiment). Analogously, for positive bias, the current is $I = I_{unp\to maj} + I_{unp\to min}$. To compare the simulations with the experimental results in Fig. 2(a), we calculate the dynamic conductances $G_{maj(min)} = \frac{dI_{maj(min)\to unp}}{dV_{dc}}$ ($V_{dc} < 0$), $\frac{dI_{unp\to maj(min)}}{dV_{dc}}$ ($V_{dc} > 0$), and then the dynamic polarization. The offset of the energy bands has been derived for transition metal FMs using first-principles band structure calculations [6,15], but it is not known for amorphous FM-I interfaces. For our calculations we use similar values as in [6,15], namely $E_{maj} \sim 2.25$ eV and $E_{min} \sim 0.5$ eV, and a barrier

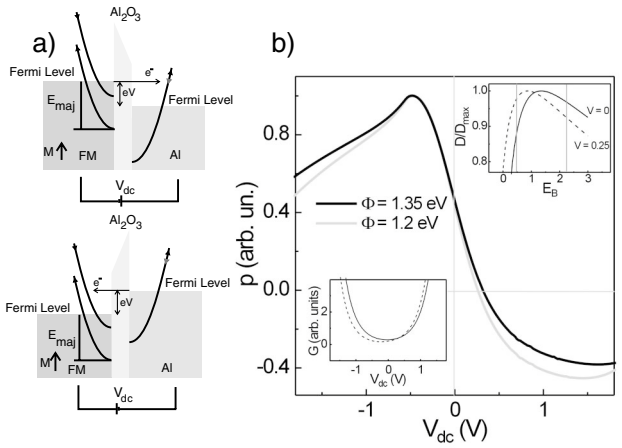

FIG. 3. (a) Schematic diagram of the source tunnel junction. Parabolic $E(k)$ curves displaced in energy represent the exchange-split majority- and minority-spin bands of the ferromagnetic electrode. Top (bottom) panel: representation of negative (positive) bias. (b) Calculated dynamic polarization p as a function of bias for $\phi = 1.35$ eV (black) and 1.2 eV (gray). The lower inset shows the dynamic conductance of the junction for the majority (solid line) and minority band (dashed line). The upper inset shows D/D_{max} as a function of E_B for different biases. In both insets, $\phi = 1.35$ eV.

with a thickness of 1.2 nm and a height ϕ equal to 1.2 eV (gray) and 1.35 eV (black) [6]. For the unpolarized band (Al) we use $E_{F,unp} = 11.7$ eV [16].

The calculated dynamic polarization [Fig. 3(b)] qualitatively follows all of the essential features of the measurements in Fig. 2 allowing us to interpret their physical origin. The bias dependence at large negative voltage is weak as in the experiments; this is a consequence of the narrow energy distribution of the injected electrons around the Fermi level (in the FM). More interesting, calculations at positive bias also show a large bias dependence as well as a sign change. The bottom panel of Fig. 3(a) shows that electrons tunneling out of the unpolarized metal face hot states in the FM. By analyzing the tunneling for the majority- and minority-spin band electrons, we conclude that the large drop in p is partially due to the fact that these hot states present a smaller ratio between the density of states of the majority and minority spins than the states around the Fermi level. This results in a suppressed spin selectivity in the tunneling.

However, from the lower inset in Fig. 3(b) it is evident that G_{min} becomes larger than G_{maj} above ~ 0.4 V, causing a sign change in p. A G_{min} larger than G_{maj} cannot be explained with just a decreasing density of states ratio. It is also necessary to note that the transmission probability D is maximized when the magnitude of the electron wave vector (in the FM) and the evanescent wave vector inside the barrier are well matched, i.e., when the electron energy measured from the bottom of the corresponding spin band in the FM ($\sim E_{min,maj} + eV_{dc}$) is comparable to the barrier

height ϕ. As $E_{\min} \neq E_{\mathrm{maj}}$, the matched state for the two spin bands in the FM will occur at different biases. The upper inset of Fig. 3(b) shows D normalized to its maximum value ($D_{\max}(V_{\mathrm{dc}})$) for electrons originating from the Al Fermi level. D is calculated for $V_{\mathrm{dc}} = 0$ and 0.25 V as a function of the energy, E_B, that defines the bottom of a given band in the FM. The actual values of E_B in our calculations, $E_{\mathrm{maj}} = 2.25$ eV and $E_{\min} = 0.5$ eV, are shown with vertical lines. D presents its maximum value at the match state, i.e., when $E_B + eV_{\mathrm{dc}} \sim \phi$. With increasing bias, the maximum moves to the left and the matching of the minority band improves ($E_{\min} + eV_{\mathrm{dc}}$ is closer to ϕ), whereas the matching of the majority band deteriorates. The relative increase in the tunneling of minority electrons is faster than expected by simple density of state considerations, and it is actually large enough to lead to a change in sign in p.

Some differences between model and experiment are observed. In particular, the measurements in Fig. 2(a) seem displaced towards positive biases as compared to the simulations in Fig. 3(b). This could be accounted by an asymmetry between the FM-Al_2O_3 and Al_2O_3-Al barrier heights that is not considered in our model [17]. On the other hand, the experimental peak which is observed close to zero bias is sharper than in the simulations. This discrepancy could be related to the ''zero bias anomaly'' in MTJs which has been attributed to scattering of electrons at defects in amorphous barriers [18], magnon excitations at the electrode-barrier [3], or a combination of both. These effects are expected to be nearly the same for positive and negative bias adding a symmetric component to p which could also account for the seeming displacement in Fig. 2(a). Comparison of Figs. 2(a) and 3(b) also suggests that a reduced barrier height in NiFe-Al_2O_3 could explain the differences with CoFe-Al_2O_3. However, other properties such as the thickness of the barrier and the band splitting at the interface could also differ in the two junction and so more research is needed to precisely establish the origin of the differences in p.

Finally, our observations are closely related to the decrease of the TMR in MTJs. As discussed above, the determination of the physical origin of the bias dependence is not trivial using MTJs themselves partly because electrons tunnel *out of* a FM cathode *into* a FM anode. Our measurements, which are able to discriminate the influence of each electrode in the tunneling polarization, suggest that the anode plays a dominant role in the TMR decrease which would be a direct consequence of the behavior of freelike tunneling electrons. They also provide a means to optimize the TMR by focusing on the design of distinct characteristics of the cathode and anode independently.

In conclusion, we measured the voltage dependence of the polarization of electrons tunneling out of and into a ferromagnet emphasizing the intrinsic asymmetry between these two processes. The polarization of electrons tunneling into the ferromagnet is strongly suppressed due to a reduced polarization for hot electron states and a spin-dependent wave-vector mismatch.

The authors thank J. U. Free and W. K. Neils for a critical reading of the manuscript. This research was supported in part by NSF Grants No. DMR-0244441 and No. NSEC-PHY-0117795 and by ONR Grant No. N00014-02-1-0055.

[1] For a review, see R. Meservey and P. M. Tedrow, Phys. Rep. **238**, 173 (1994).
[2] M. Julliére, Phys. Lett. **54A**, 225 (1975); J. S. Moodera *et al.*, Phys. Rev. Lett. **74**, 3273 (1995); T. Miyazaki and N. Tezuka, J. Magn. Magn. Mater. **139**, L231 (1995).
[3] S. Zhang *et al.*, Phys. Rev. Lett. **79**, 3744 (1997); J. S. Moodera *et al.*, Phys. Rev. Lett. **80**, 2941 (1998).
[4] D. Nguyen-Manh *et al.*, Mater. Res. Soc. Symp. Proc. **492**, 319 (1998); M. Sharma *et al.*, Phys. Rev. Lett. **82**, 616 (1999); J. M. de Teresa *et al.*, Science **286**, 507 (1999).
[5] P. Mavropoulos *et al.*, Phys. Rev. Lett. **85**, 1088 (2000).
[6] A. H. Davis and J. M. MacLaren, J. Appl. Phys. **87**, 5224 (2000).
[7] F. Montaigne, M. Hehn, and A. Schuhl, Phys. Rev. B **64**, 144402 (2001).
[8] M. Johnson and R. H. Silsbee, Phys. Rev. Lett. **55**, 1790 (1985); Phys. Rev. B **37**, 5312 (1988).
[9] M. Johnson and R. H. Silsbee, Phys. Rev. B **35**, 4959 (1987).
[10] F. J. Jedema *et al.*, Nature (London) **416**, 713 (2002).
[11] For further details, see S. O. Valenzuela and M. Tinkham, Appl. Phys. Lett. **85**, 5914 (2004).
[12] Note that the dynamic polarization measures contributions from electrons within a narrow energy range for each bias voltage, whereas the standard current polarization includes contributions from all electrons.
[13] The reduction of the switching field seen in Fig. 2(b) occurs abruptly at biases above 50 mV. For higher biases, the switching field stays constant suggesting that the reduction is due to current (or Oersted field)-induced depinning of domain walls which facilitates the switching. See, e.g., M. Tsoi *et al.*, Appl. Phys. Lett. **83**, 2617 (2003). Heating does not seem to be a factor in the measurements. This is reflected in constant switching fields at high bias and in an invariant bias dependence of the normalized p for different temperatures and for different distances between the ferromagnets.
[14] K. H. Gundlach, Solid-State Electron. **9**, 949 (1966).
[15] M. B. Stearns, J. Magn. Magn. Mater. **5**, 167 (1977).
[16] Results are qualitatively independent of $E_{F,\mathrm{unp}}$ which was then chosen to be equal to the Fermi energy of Al.
[17] W. F. Brinkman *et al.*, J. Appl. Phys. **41**, 1915 (1970).
[18] J. Zhang and R. M. White, J. Appl. Phys. **83**, 6512 (1998); H. F. Ding *et al.*, Phys. Rev. Lett. **90**, 116603 (2003).